

650 MHz Elliptical Cavity Performance Degradation Induced by Magnetic Field of a Test Coil

T. Khabiboulline, D. Sergatskov, I. Terechkin

I. Introduction

First tests of 1-cell 650 MHz elliptical cavities designed for PX linac have demonstrated that the quality factor of the cavities can exceed $5 \cdot 10^{10}$. To rely on this high quality factor in the cavities built for use in the linac, some features of cryomodule design related to magnetic shielding must be re-evaluated. As the initial step to this re-evaluation, a reliable model for possible magnetic-field-induced quench degradation must be used. Approach to building this model was first formulated in [1] for the case of a 1.3 GHz elliptical cavity with further studies made in [2], [3], and [4], where a criterion of acceptable magnetic field was suggested and verified by corresponding measurements. Those measurements were made with the use of a superconducting coil that generated magnetic field in the vicinity of superconducting RF structures under study. Methodology of the approach to the quench degradation analysis is also described in [5].

Main parameters of the tested 650-MHz 1-cell cavity are listed below:

- | | |
|--|--|
| 1. Geometrical beta | 0.9 |
| 2. Operating gradient G_{acc} | 17 MV/m; |
| 3. Max surface electric field at operating gradient | 33.7 MV/m; |
| 4. Maximum magnetic field at operating gradient | 63 mT; |
| 5. Stored energy W_0 at at operating gradient | 25 J; |
| 6. R_{sh}/Q | 127.2 Ohm |
| 7. Quality factor at 6 MV/m | $5 \cdot 10^{10}$ |
| 8. $K_H = W_0/H^2$ on the equator of the cavity | $9.85 \cdot 10^{-9} \text{ J}/(\text{A}/\text{m})^2$ |
| 9. Magnetic field distribution on the surface of the cavity is close to uniform. | |

Based on the data in this table, a ratio of the maximum field on the surface to the accelerating gradient

$$K_G = H_m/G_{acc} = 2950 \text{ A/MV.}$$

The energy stored in the cavity at any gradient can be found by using the next expression:

$$W = K_H * K_G^2 * G_{acc}^2$$

II. Test setup

The cavity was tested in the VTS equipped with two magnetic shields to reduce environmental magnetic field [6]. Fig. 1 shows magnetic field distribution along several lines parallel to the vertical axis of the VTS at room temperature (before cooling down). At the location of the tested cavity (3.5 m to 4 m from the top flange of the VTS), the magnetic field does not exceed 1.5 mG ($1.5 \cdot 10^{-7} \text{ T}$). As the magnetic properties of the inner shield of the VTS,

which is made of Cryoperm10, are optimized for the 4 K temperature, even smaller magnetic field can be expected after the cooling down.

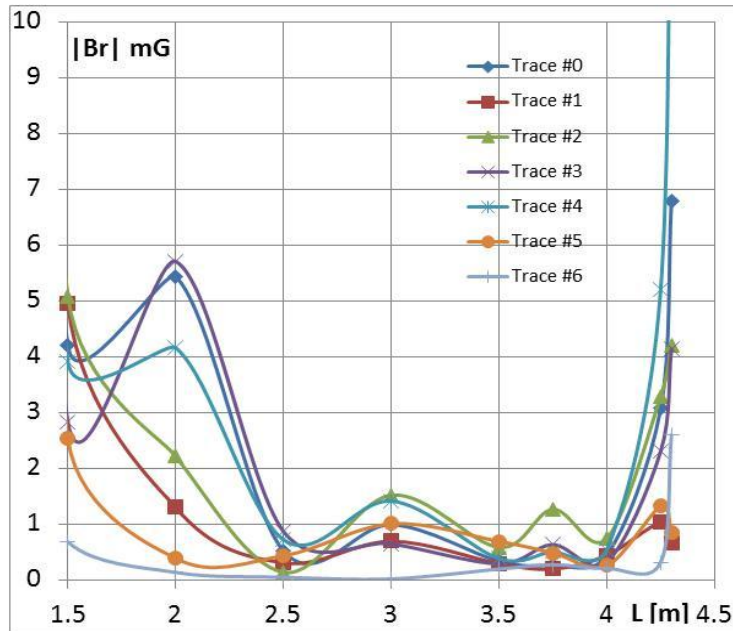


Fig. 1. Magnetic field in the VTS before cooling down.

Layout of the cavity and the test coil in the VTS is shown in Fig. 2.

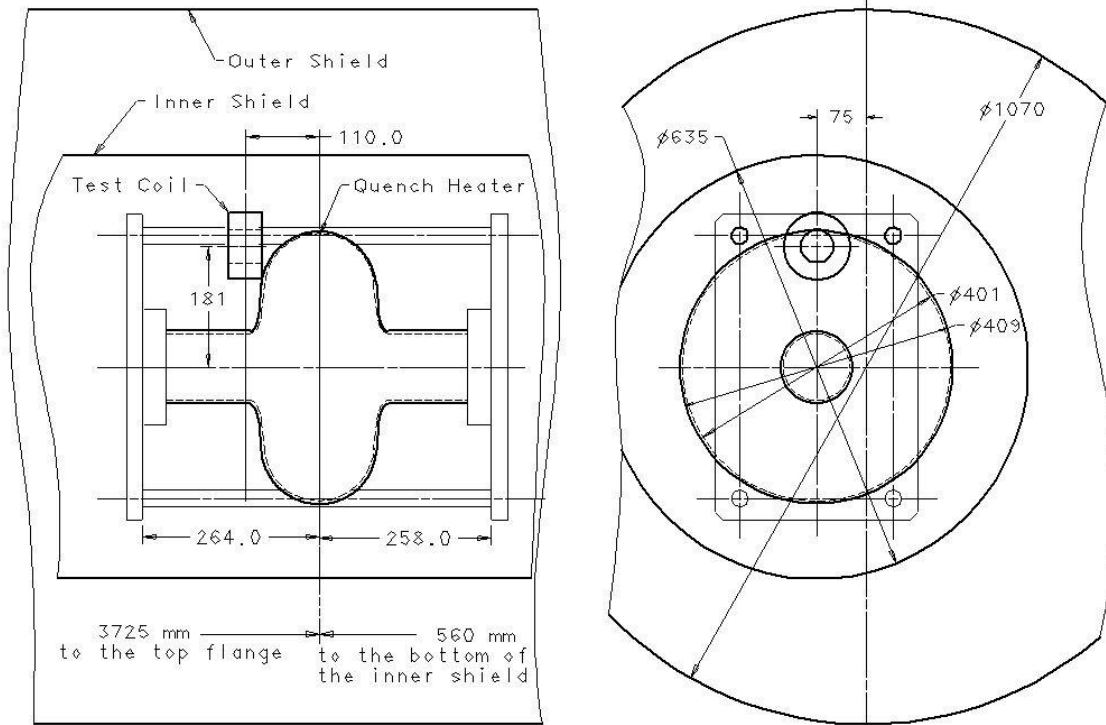


Fig. 2. 650 MHz elliptical 1-cell cavity and test coil in the VTS

Photo in Fig. 3 shows relative position of the test coil and the cavity.

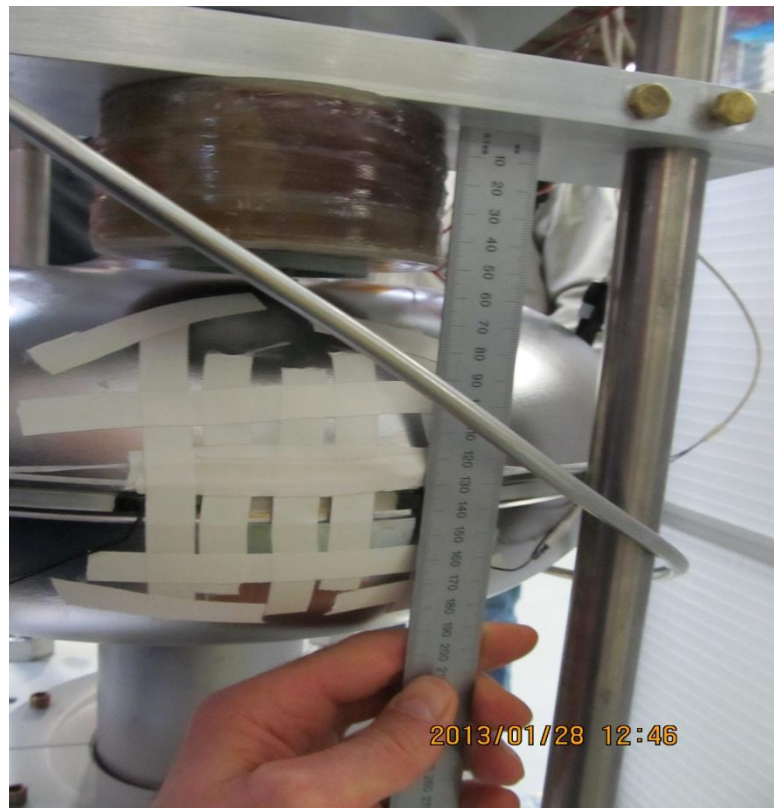


Fig. 3. Coil and quench heater position on the cavity: distance between the mid-planes of the cavity and the coil is 110 mm.

Superconducting coil used for the test is identical to that used in [2] and [3]. With known position and orientation of the coil, magnetic field can be readily found; this position is defined as a trade-off between two trends: a desire to place the coil closer to the quench spot (that is to the quench heater position) and a necessity to place it as far from the magnetic shield as possible to mitigate shield magnetization. As it was done in [3], a 5 Ω MINCO film resistor was used as a heater; it was activated by using Heater Firing Unit (HFU) available at MT department of TD; the HFU was configured to have the storage capacitance value $C = 2400 \mu\text{F}$.

To find magnetic flux trapped in the cavity wall during quenching, one needs to know the size of a normally conducting opening in the superconducting wall of the cavity. The next chapter describes results of corresponding modeling.

III. Development of normally conducting opening during quenching

Quench propagation modeling was made using axially symmetric 2D geometry similar to how it was made in [1]; the only significant difference in the model was different thickness of the Nb sheet, which in this case is 4 mm. Approximation of relevant material properties was made similar to how it was done in [1], that is by using interpolation function and lookout tables; below some of these functions are provided.

- Specific heat of Nb:

$$C_p(T) = C_{p0} \cdot (1 - \exp(-1.5 \cdot (T/80)^2)) \quad \text{with } C_{p0} = 220 \text{ J/(kg}\cdot\text{K)}$$

- Thermal conductivity of Nb:

$$\begin{aligned} k(T) &= k_0 && \text{if } T < 1 \text{ K,} \\ k(T) &= k_0 \cdot T && \text{if } 1 \text{ K} < T < 9.5 \text{ K,} \\ k(T) &= 9.5 \cdot k_0 && \text{if } 9.5 \text{ K} < T < 18 \text{ K,} \\ k(T) &= k_0 \cdot (1.656 + 7.844 \cdot (18/T)^{2.4}) && \text{if } T > 18 \text{ K,} \end{aligned}$$

with $k_0 = 32 \text{ W/(m}\cdot\text{K)}$.

- Heat transfer coefficient into liquid helium with background temperature 2 K (LHe-2):

$$h(T) = 10 \cdot T + 6000/T \quad \text{in [W/(m}^2\cdot\text{K)]}.$$

- Resistivity of normally conducting Nb as a function of the temperature :

$$\rho(T) = \rho_0 \cdot (1 + 5 \cdot 10^{-4} \cdot T + 2.2 \cdot 10^{-3} \cdot T^2) \quad \text{with } \rho_0 = 7 \cdot 10^{-10} \text{ Ohm}\cdot\text{m}.$$

Although different (and probably more precise) expressions exist to parameterize the resistivity of Nb (e.g. see [8]), this simple one works well at $T > 9.2 \text{ K}$. Resistivity of normally conducting Nb at 2 K can be found if the purity of Nb expressed in terms of RRR is known:

$$\rho(2\text{K}) = \rho(300\text{K})/\text{RRR},$$

where $\rho(300\text{K}) = 1.45 \cdot 10^{-7} \text{ Ohm}\cdot\text{m}$ [9]. Knowing resistivity of normally conducting Nb, the skin depth δ can be found using general (classical) expression

$$\delta = (\rho/(\pi \cdot \mu_0 \cdot f))^{1/2}$$

The surface resistance of normally conducting Niobium can be found using the expression:

$$R_s = \rho/\delta.$$

Anomalous skin effect for Nb can be neglected as it becomes significant only when the mean free path of electrons l becomes comparable and larger than the classical skin depth. For Nb, $l \approx 10^{-3} \mu\text{m}$; the skin layer thickness for normally conducting RRR300 Nb at 650 MHz and 2 K ($\rho = 4.83 \cdot 10^{-10} \text{ Ohm}\cdot\text{m}$) $\delta = 0.43 \mu\text{m}$, so: $l \gg \delta$. As it is shown in [9], the value of RRR, beside it being altered during fabrication and subsequent heat treatments, varies along the cavity surface. In our case RRR = 300 was found to be consistent with the cavity performance at low temperature.

As it was done in [3], initiation of a quench is made by using a resistive quench heater. During modeling, this heat is represented by a heat flux into the surface with the initial heat flux density $\sim 2 \cdot 10^6 \text{ W/(m}^2\cdot\text{K)}$ and the time constant $\sim 10 \text{ ms}$. Modeling showed that at the 17 MV/m gradient, the threshold heat flux is $1.2 \cdot 10^6 \text{ W/m}^2$; with the 5 cm^2 of the effective surface area of the heater, this leads to the requirement of having $\sim 6 \text{ J}$ deposited in the wall before quench is initiated. This requirement can be met if the voltage of the HFU is higher than 70 V. During test we have found that this voltage must be higher than 120 V.

Main parameter during quench propagation (QP) modeling is the initial energy W_0 stored in the cavity before quench, which is a function of the accelerating gradient. Fig. 4 shows how the radius of the normally conducting zone (found by modeling) changes in time for different values of the accelerating gradient.

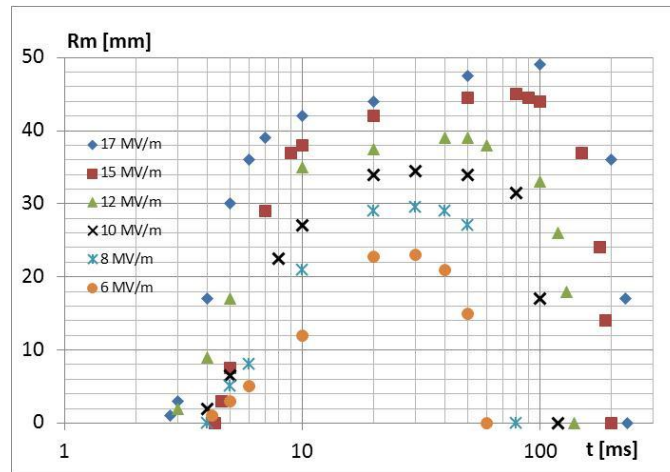


Fig. 4. Development of the normally conducting opening in the 4-mm wall of the cavity for different values of the accelerating gradient.

Table 1 shows correspondence between the accelerating gradient and the stored energy W_0 for a 1-cell 650 MHz $\beta=0.9$ elliptical cavity.

Table 1. Energy stored in the cavity for different values of the accelerating gradient

| G (MV/m) | 6 | 8 | 10 | 12 | 15 | 17 | 20 |
|-----------|-----|------|------|-------|-------|----|----|
| W_0 (J) | 3.1 | 5.54 | 8.65 | 12.46 | 19.46 | 25 | |

Fig. 5 shows how the size of the opening depends on the initially stored energy W_0 . This dependence can be quite accurately expressed by the next expression:

$$R_m[\text{mm}] = 16.7 \cdot (W_0[\text{J}])^{1/3}$$

In [3] the energy dependence for the 325 MHz spoke-type cavity was approximated by a linear function in the limited range of the stored energy. It can also be approximated in the total range of the energies by using the expression $R_m[\text{mm}] = 17.0 \cdot (W_0[\text{J}])^{1/3}$.

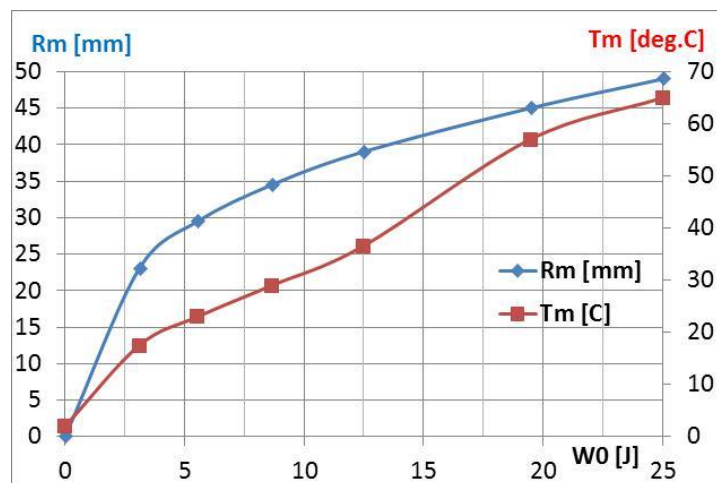


Fig. 5. Radius of the normally conducting opening and the maximum temperature as functions of the stored energy.

Red trace in Fig. 5 shows the maximum temperature of Nb.

As the size of the normally conducting opening in the superconducting wall of the cavity is known, evaluation of the trapped magnetic flux is straightforward, and can be made for any initial energy in the cavity. This provides information needed for calculation of the field-induced degradation of the cavity performance.

IV. Field-induced degradation of the cavity performance

Following [2], we can introduce the “Field-Induced” portion of the quality factor:

$$Q_{FI} = 2 \cdot \omega \cdot K_H / (R_s \cdot S_n), \quad /1/$$

At $f = 650$ MHz, with $K_H = 9.85 \cdot 10^{-9}$ J/(A/m)², and at 2 K ($\rho = 4.83 \cdot 10^{-10}$ Ohm·m) the surface resistance $R_s|_{2K} = 1.1 \cdot 10^{-3}$ Ohm.

Total surface area S_n of the normally-conducting zones associated with the trapped flux in a superconducting wall can be evaluated (as in [1]) by using the expression

$$S_n = \pi \cdot \xi_0^2 \cdot \Phi / \Phi_0,$$

where $\xi_0 = 3.9 \cdot 10^{-8}$ m and $\Phi_0 = 2 \cdot 10^{-15}$ T·m².

By substituting all the known values in /1/, we can write down:

$$Q_{FI} = 3.06 \cdot 10^4 / \Phi$$

For the test geometry in Fig. 2, the trapped flux Φ was found by using direct 3D magnetic modeling (as was done in [2]); it is fully defined by the coil current.

Fig. 6 shows distribution of magnetic field in the vicinity of the normally conducting opening with 1 A coil current. One can see penetration of the field in the opening in the superconducting wall. The maximum magnetic field on the surface of the cavity is ~500 Gs, which is well below the H_{c2} value (which is ~2000 Gs for Nb).

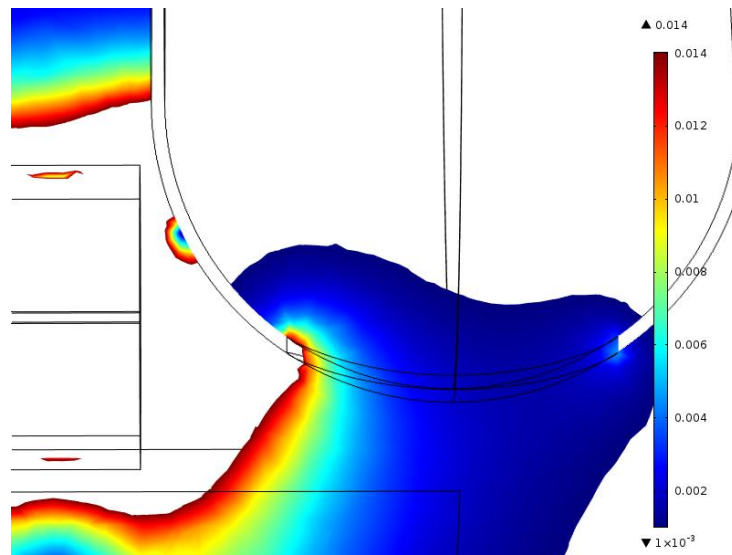


Fig. 6. Field map at 1 A current in the test coil.

As the trapped flux depends on the size of the normally conducting opening, which in turn depends on the energy stored in the cavity (or the initial value of accelerating gradient), it has sense to make modeling for the values of the accelerating gradient observed during testing, which was performed on January 29, 2013. As time available for this specific test was scarce (the goal of the main part of the test was to obtain information about cavity performance), only a small part of the initial program was implemented. Nevertheless, obtained results, presented in the next chapter, compare well with findings made earlier in [1], [2], and [3].

V. Summary of the test and comparison with the modeling

In comparison with the test procedure we used in [2] and [3], more simple way has been chosen to save time: no quench annealing procedure was applied after each quench event. Instead this procedure was applied after each series of quenches with constant accelerating gradient. This change was made based on the previous experience when full, or at least partial, restoration of the cavity performance was observed during quenching without magnetic field. We assumed this time that with each new quenching the old history is erased, and the new history starts. Solid line in Fig. 7 shows calculated quality factor of the cavity with the accelerating gradient $G_{acc} = 20$ MV/m; it drops as the current in the test coil (and the trapped flux) increases. Squares in the same graph represent test results.

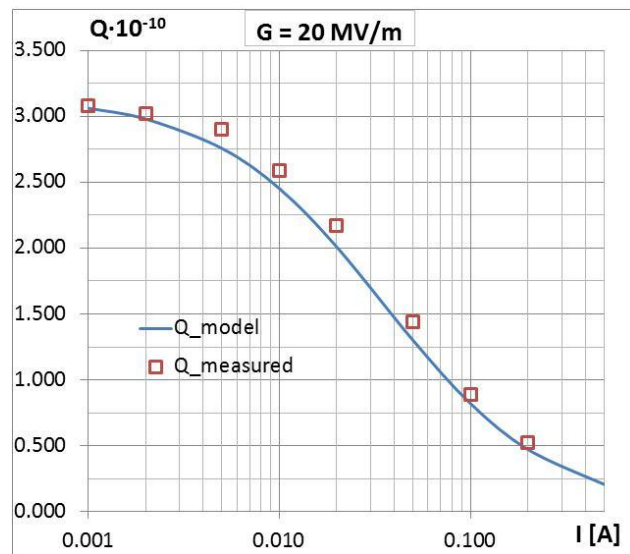


Fig. 7. Cavity performance degradation at $G = 20$ MV/m. 100% magnetic flux trapping efficiency is assumed.

The analysis summarized in this figure was made assuming 100% flux trapping efficiency. Taking into account our previous experience we can guess that at higher excitation current part of the trapped flux cannot be expelled from the surface during quenching as it drifts out of the heated zone, so one should expect that at higher test coil excitation current the measured values of Q must be lower than what the model would show; we do not see this in the figure though. If a

smaller part of the magnetic flux is trapped, the graph representing modeling results will change correspondingly; in Fig. 8 modeling results correspond to 70% of the flux trapped. Here we definitely see that at sufficiently high excitation current the measured quality factor due to the trapped flux is lower than what the modeling predicts.

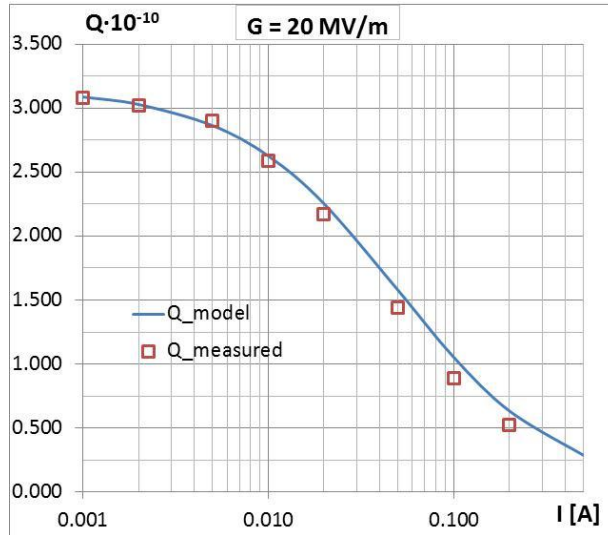


Fig. 8. Cavity performance degradation at $G = 20$ MV/m. 70% of the magnetic flux trapped.

We need to recognize though that there is a standing opinion among scientists studying limiting processes in superconducting RF cavities that we should expect the flux trapping efficiency close to 100% [10], which is consistent with previously made studies (e.g. in [11]).

Results of the quench annealing procedure applied after testing the cavity with $G = 20$ MV/m are shown in Fig. 9.

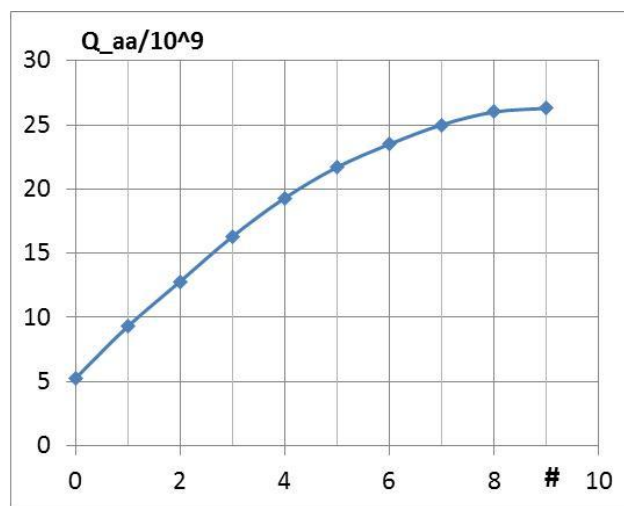


Fig. 9. Quench annealing process after the $G = 20$ MV/m test

The graph in the figure shows how the quality factor of the cavity changes during heater-induced quenching without magnetic field ($I = 0$, the so-called quench annealing process). Values on the X-axis represent the number of quenches made. The quality factor is restored to $\sim 84\%$ of the initial value, and the annealing process is close to saturation, which is a reflection of the fact mentioned above: magnetic flux drifts out of the heated area and cannot be expelled from the superconducting wall.

The $2.6 \cdot 10^{10}$ quality factor at 20 MV/m was the starting point for the next phase of the test where the gradient was set 10 MV/m; with this twice as low gradient the quality factor increased to $Q = 3.9 \cdot 10^{10}$. Results of the test are summarized in Fig. 10; as earlier, the line shows the trend found by modeling, and the squares represent what was measured during the test.

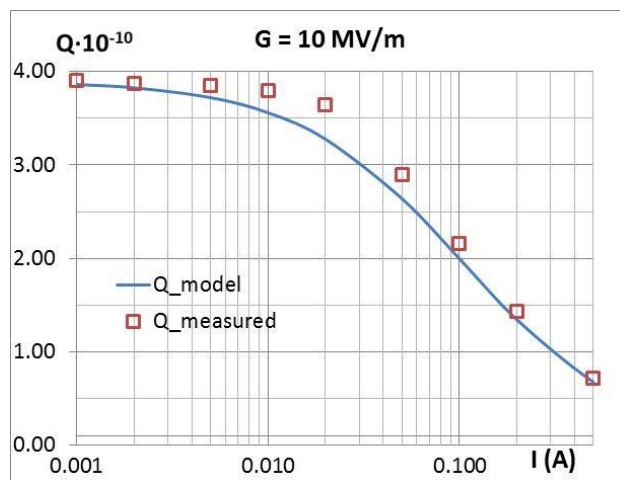


Fig. 10. Cavity performance degradation at G = 10 MV/m. 100% of the magnetic flux trapped.

In Fig. 11, results of the modeling with 70% of the flux trapping efficiency are shown for comparison.

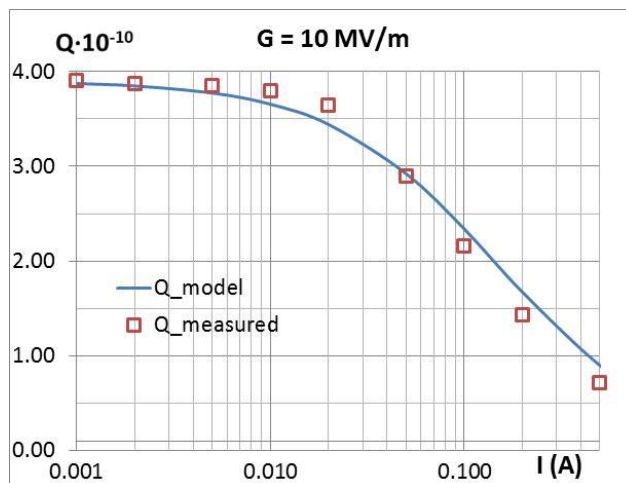


Fig. 11. Cavity performance degradation at G = 10 MV/m. 70% of the magnetic flux trapped.

Results of the quench annealing procedure applied after the $G = 10$ MV/m test are shown in Fig. 12. To accelerate the quench annealing process, after quench #6 the accelerating gradient was set to 20 MV/m. This resulted in lower Q , but larger size of the normally conducting opening during quenching, in accordance with Fig. 5. After just one quench at 20 MV/m, the quality factor was restored to the initial value of $3.9 \cdot 10^9$.

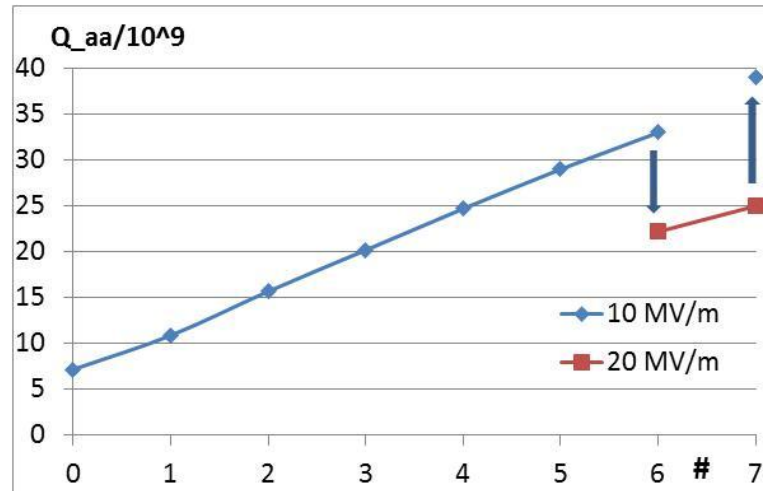


Fig. 12. Quench annealing process after the $G = 10$ MV/m test

IV. Conclusion

650 MHz elliptical cavity performance degradation induced by magnetic field was studied using previously developed method. Results of the study are consistent with what was found earlier for cavities of different shapes and frequencies. As during this set of tests we could rely on the previous experience, the basic assumption of a 100% magnetic flux trapping efficiency accepted in [3] was verified. In this case, the assumption of a 70% field trapping efficiency results in a better correspondence between the modeling prediction and the measurement results. Although this may contradict to what was found in [11], some recent studies show that the efficiency of flux trapping can change depending on the quality of Nb and on the used heat treatment process [12].

References:

1. I. Terechkine, “Modeling Quench Propagation in Superconducting cavity Using COMSOL”, FNAL TD note TD-11-019, Dec. 07, 2011.
2. T. Khabiboulline, et al, “Superconducting Cavity Quenching in the presence of Magnetic Field”, FNAL TD note TD-11-020, Dec. 30, 2011.
3. T. Khabiboulline, et al, “SSR1 Cavity Quenching in the Presence of Magnetic Field”, FNAL TD note TD-12-007, June 18, 2012.
4. T. Khabiboulline, et al, “Acceptable Level of Magnetic Field on the Surface of a Superconducting RF Cavity”, FNAL TD note TD-12-008, June 25, 2012.
5. T. Khabiboulline, et al, “Superconducting Cavity Performance Degradation after Quenching in Static Magnetic Field”, COMSOL-2012 conference proceedings, Boston, Oct.03 – 05, 2012.
6. C. Ginsburg, et al, “Magnetic Shielding for the Fermilab Vertical Cavity Test Facility”, FERMILAB-CONF-08-348-TD, FNAL, 2008.
7. H. Padamsee, J. Knobloch, and T. Hays, RF Superconductivity for Accelerators”, Wiley&Sons, Inc, 1998, p. 59
8. G. W. Webb, “Low-Temperature Electrical Resistivity of Pure Niobium”, Physical Review, vol. 181, Issue 3, pp. 1127-1135.
9. H. Safa, et al, “RRR mapping of the SRF cavities by a magnetometric method”, 1997 Workshop on RF Superconductivity, proceedings, pp. 864 – 872.
10. A. Romanenko, private communication.
11. C. Vallet, et al, “Flux Trapping in Superconducting Cavities”, EPAC-92, proc. p. 1295.
12. S. Aull, O. Kugeler, J. Knobloch, “Trapped Magnetic Flux in Superconducting Niobium Samples”, Phys. Rev. Special Topics – Accelerators and Beams, **15**, 062001-1 (2012).